

Utah State University

DigitalCommons@USU

---

Physics Capstone Projects

Physics Student Research

---

Summer 2013

## Studying Light Pollution in and Around Tucson, AZ

Rachel K. Nydegger  
*Utah State University*

Follow this and additional works at: [https://digitalcommons.usu.edu/phys\\_capstoneproject](https://digitalcommons.usu.edu/phys_capstoneproject)



Part of the [Physics Commons](#)

---

### Recommended Citation

Nydegger, Rachel K., "Studying Light Pollution in and Around Tucson, AZ" (2013). *Physics Capstone Projects*. Paper 3.

[https://digitalcommons.usu.edu/phys\\_capstoneproject/3](https://digitalcommons.usu.edu/phys_capstoneproject/3)

This Report is brought to you for free and open access by the Physics Student Research at DigitalCommons@USU. It has been accepted for inclusion in Physics Capstone Projects by an authorized administrator of DigitalCommons@USU. For more information, please contact [digitalcommons@usu.edu](mailto:digitalcommons@usu.edu).



# Studying Light Pollution in and around Tucson, AZ

## KPNO REU Summer Report 2013

Rachel K. Nydegger

*Utah State University, Kitt Peak National Observatory,  
National Optical Astronomy Observatory*

Advisor: Constance E. Walker

*National Optical Astronomy Observatory*

### ABSTRACT

Eight housed data logging Sky Quality Meters (SQMs) are being used to gather light pollution data in southern Arizona: one at the National Optical Astronomy Observatory (NOAO) in Tucson, four located at cardinal points at the outskirts of the city, and three situated at observatories on surrounding mountain tops. To examine specifically the effect of artificial lights, the data are reduced to exclude three natural contributors to lighting the night sky, namely, the sun, the moon, and the Milky Way. Faulty data (i.e., when certain parameters were met) were also excluded. Data were subsequently analyzed by a recently developed night sky brightness model (Duriscoe (2013)). During the monsoon season in southern Arizona, the SQMs were removed from the field to be tested for sensitivity to a range of wavelengths and temperatures. Future work might include further validation of the accuracy and precision of these devices by comparing to the Suomi Visible Infrared Imaging Radiometer Suite (VIIRS) as well as the Globe at Night (GaN) data.

### 1. Introduction

Though the view of city lights is considered a modern beauty, it is the cause of an assortment of negative effects (Navara & Nelson. (2007)). Most street lights emit light radially, sending large portions of the light into the sky, leaving the ground dim. The excess light - light pollution - directed upwards destroys our ability to view beauty of the night sky and repre-

sents a loss of energy and money. Animals are often attracted to or repelled by light, disrupting their hunting and mating patterns as well as other behaviors. Similarly, human health is negatively impacted by the the change in circadian rhythm. Studies have shown that women who are exposed to light while working at night have a much higher risk of breast cancer (Hansen (2001)). Other negative effects of light pollution include depression, insomnia, and

other forms of cancer.

Quantifying the light pollution with housed data-logging Sky Quality Meters (SQMs) can give a sense of how much excess light there is in Tucson, and therefore provides a starting point to address this issue. These meters have a FOV FWHM of  $20^\circ$  and are able to collect data either automatically based on time and darkness or manually through a USB connection. For this project, each SQM takes data every five minutes whenever the sky is darker than  $12 \text{ mag/arcsec}^2$ . To better analyze the data collected by these devices, the sensitivity of the devices was tested in regard to various visible wavelengths. Results from these tests called for inspection of the filter inside each SQM and the glass atop the housing of the device.

To focus analysis on anthropogenic light pollution, raw data are reduced through a series of python scripts that remove readings taken when the moon, sun, or Milky Way is overhead. These scripts also remove erroneous readings. The goal of this paper is to present and discuss spatial and temporal trends in the anthropogenic sky glow over Tucson from 2012-2013 using these reduced data.

## 2. Laboratory Testing

To measure the effect outdoor lighting in Tucson has on light pollution, one SQM is placed at each of the following sites: the National Optical Astronomy Observatory (NOAO), each cardinal point at the outskirts of Tucson, Kitt Peak, Mt. Lemmon, and Mt. Hopkins. Population varies greatly by location, thereby changing the outdoor lighting and, consequently, the sky brightness. Observatories often use low-pressure sodium lights, whereas Tucson contains LED sources, the SQM detector is not as sensitive to. Therefore, knowing

how the meter responds to specific wavelengths of light assists in interpreting light pollution data.

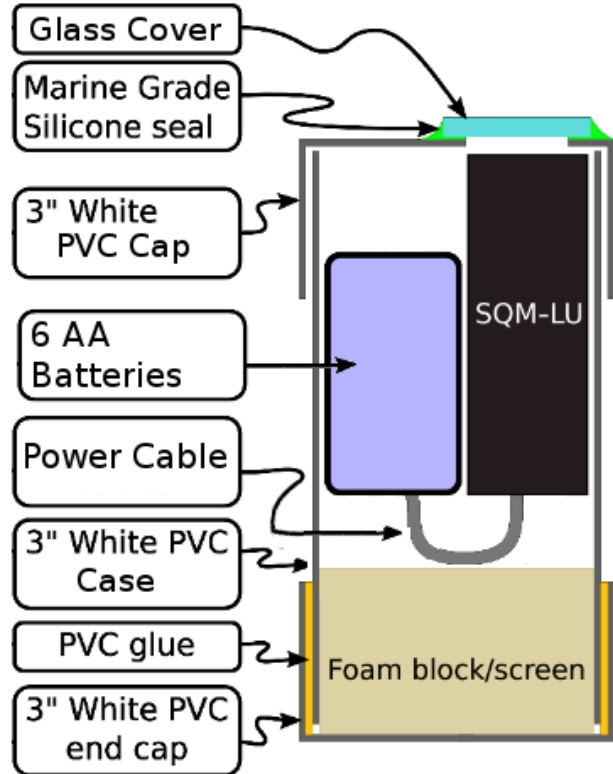


Fig. 1.— Diagram of an SQM

### 2.1. Wavelength Sensitivity

In order to characterize readings from each SQM, the meters were placed within an integrating sphere to ensure uniform exposure from sources of varying wavelength. Diodes emitting light of wavelengths 365 nm, 470 nm, 570 nm, 655 nm, 770 nm, 850 nm, and 950 nm were used to represent the visible spectrum. The source outputs were held at constant voltages corresponding to SQM readings of approximately  $20 \text{ mag/arcsec}^2$ , as described in Table 1. Voltage was reported by a reference sensor inside of the integration sphere. Once the output voltage was stabilized, 25 readings were taken for each SQM with and without housing, cover, and glass filter (see Fig. 1

for a visual representation of these components). Unihedron, the manufacturer of this device, reports that the first reading is often erroneous due to temperature calibration (Unihedron (2013)), and so it should be removed for the sake of validity. As readings were collected every second, the first five readings were taken out of each data set.

$\lambda$ (nm)	Voltage (eV)
365	.0400
470	.0435
570	.0810
655	.1030
770	.1160
850	.1190
950	.1470

Table 1: Source output was kept constant to ensure valid data comparison for each wavelength. Output was varied according to wavelength to avoid over-saturation of the SQM detector.

The intensity readings in the integration sphere were dependent upon which each SQM was used, leading to the discovery that the reflectivity of the SQM caps varied. The meters were exposed to different levels of UV radiation at their respective sites, causing the housing of some devices to yellow more than others (see Fig. 2). To address this inconsistency, light masks were made to cover all of the caps except for the openings during laboratory testing. Data collected during this time were not used for error analysis. Eventually, the housings of these SQMs will be coated on the outside with a glossy white paint to prevent UV yellowing and maintain a cool temperature within the case. To reduce light scattering within the housing, the inside of the case will be coated with a dull black paint.

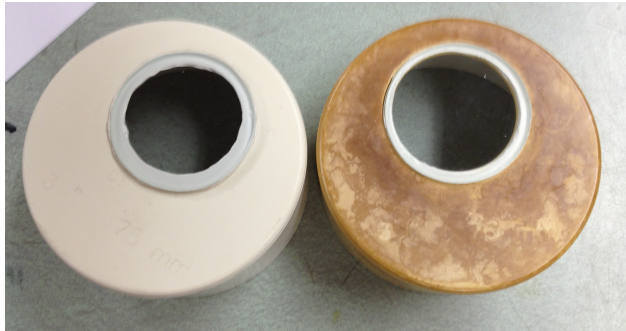


Fig. 2.— Weatherproof housing units have varying levels of reflectivity due to UV yellowing in the field.

The HOYA-CM500 filter located within the meter should have no transmission between 730 nm and 1020 nm (Hoya-Optics (2008)), but readings of roughly 20 mag/arcsec<sup>2</sup> were obtained for wavelengths within this range. These readings, however, required a higher source output voltage to achieve. This finding prompted further testing on the filter, outlined in section 2.2.

Table 2 provides the results from two of the six test combinations for each SQM and wavelength. In test 'A', the SQM alone collected results, whereas test 'B' included the glass filter, housing, and cover. The presence of these accessories darkened SQM readings by approximately 0.1 mag/arcsec<sup>2</sup>.

The manufacturer of these devices reports a zero-point offset of up to  $\pm 0.1$  mag/arcsec<sup>2</sup> (Unihedron (2013)), which is much greater than the 95% confidence range presented in the table. Therefore, the standard deviations are not indicative of the accuracy of the measurements, but of the precision.

## 2.2. CM500 Filter

The filter inside of the SQM should prevent exposure to wavelengths longer than

700 nm, but laboratory results showed that near infrared sources are detected. Fig. 3 shows the standard deviation of measurements taken for each of eight wavelength sources, thereby giving a measure of SQM agreement for each wavelength. Between 365 nm and 570 nm, the meters are in good agreement. The standard deviation increased when the SQMs were exposed to longer wavelengths, which prompted examination of the CM500 filter.

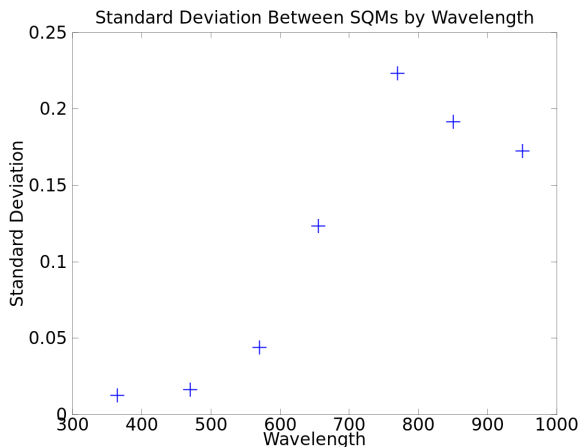


Fig. 3.— Standard deviation of readings between each SQM at each wavelength tested.

With the cooperation of the manufacturer, one of the SQMs was opened in order to inspect the filter. As seen in Fig. 4, the blue-green (square) filter is held within a plastic case; the detector would be at the top of the plastic case as shown and the lens is seen at the bottom. There is a chance that the filter is too small for the detector so that light is effectively leaking around it. The leak is made worse by the fact that the detector is tilted with respect to the optical axis. The large standard deviation between SQMs in measurements for wavelengths greater than 700nm indicates an inconsistency in the effectiveness of the filtering apparatus in each SQM.

While the manufacturer of this filter reports that the filter transmits photons between 1000 nm and 4000 nm (Hoya-Optics (2008)), this is not an area of concern as the SQM’s detector, a TSL237, has a spectral responsivity between 300 nm and 1100 nm (TAOS (2007)).



Fig. 4.— Filter from inside the SQM stationed at NOAA.

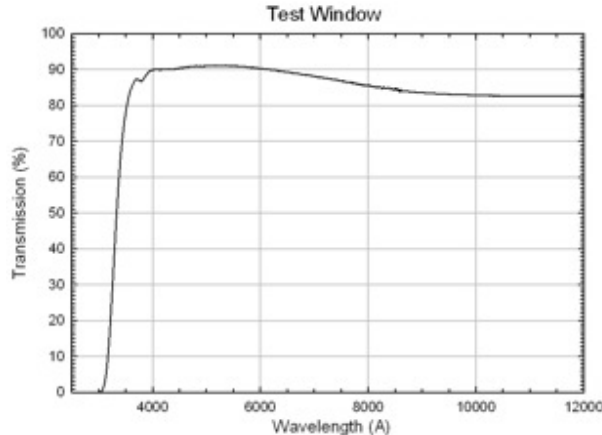


Fig. 5.— Transmission curve of the glass filter analyzed by Dick Joyce

### 2.3. Glass Cover Filter

Results from aforementioned testing showed that the glass filter consistently affected the light integration of the SQM. The transmission curve found for this glass cover illustrates a loss of roughly 10%

around 400 nm, as seen in Fig. 5. The transmission steadily drops down to about 83% around 900 nm. Data with and without glass taken during the wavelength sensitivity testing were compared and produced a trend that is in agreement with the transmission curve (see Fig. 6).

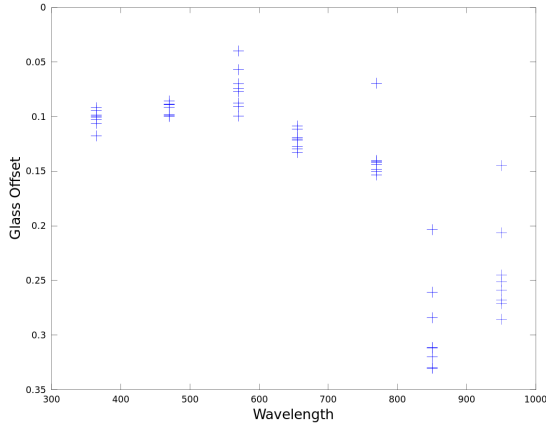


Fig. 6.— Offset between tests taken with the SQM alone and with glass covering the detector.

### 3. SQM Data

While the SQMs are at their respective sites, they begin collecting data every five minutes once the sky is darker than 12 mag/arcsec<sup>2</sup>. The SQMs are able to accurately measure sky brightnesses as dark as 24 mag/arcsec<sup>2</sup>. After the data are retrieved, they are reduced by a series of python scripts. While these newly created codes are used locally in Tucson and the surrounding areas, there is potential for implementation into a Globe at Night (GaN) GUI to assist citizen science studies in anthropogenic sky glow. After reduction, the data are analyzed for spatial and temporal trends.

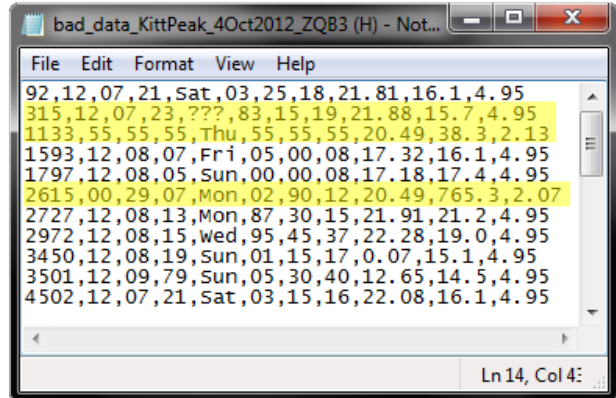


Fig. 7.— A file of faulty data from Kitt Peak.

### 3.1. Data Reduction

Each SQM reports the time a measurement was taken, the sky brightness value, the temperature, and the voltage. When the voltage of the device is too high, it automatically prevents the use of faulty data by replacing the data with fives (seen in the second highlighted row of Fig. 7); however, most other errors in the data are salvageable. Occasionally, the data will be saved with unrealistic years, days, hours, minutes, SQM readings, etc. Often, the errors can be identified by comparing to the lines of data recorded five minutes prior and afterwards and consequently can be fixed. Others, specifically the faulty SQM readings, must be removed from the data. The first script in the pipeline amends usable data and creates a file listing the bad data to be investigated at a later time.

Once erroneous data are fixed or removed, any remaining data taken during twilight or while the sun, moon, or Milky Way are overhead are removed via secondary scripts for analysis. This is done in order to help isolate the anthropogenic contribution to sky glow.

To assess the the validity of the reduction, and ensure that the integrity of the

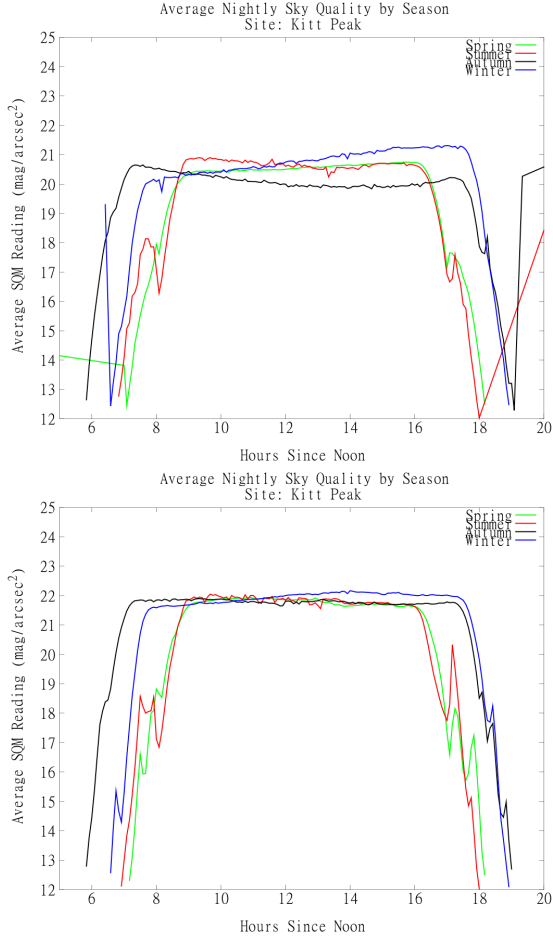


Fig. 8.— The average seasonal raw (top) and reduced (bottom) data collected from Kitt Peak

data is preserved, comparisons are made between the pre and post faulty measurement reduction such as in Fig. 8. These plots show the average night of each season. Fig. 8b shows the SQM measurements have much less variation after reduction.

### 3.2. Sky Brightness Model

To further focus on the contribution of artificial lights, twilight is removed and compared to the results of Dan Duriscoe’s sky brightness model. The National Park Service uses a silicon-based device to measure light pollution as well, and Dan

Duriscoe’s model addresses the distinction between natural and artificial light pollution for this device (Duriscoe (2013)). Therefore, this model provides a good representation of light pollution measurements taken by an SQM. This model uses information about the position of the moon, Milky Way, stars, and planets based on time of an SQM reading and uses latitude, longitude, airglow, and degree from zenith to determine what the natural sky glow should be in terms of nanolamberts as well as mag/arcsec<sup>2</sup>. Fig. 9 compares the average predicted natural sky brightness at Mt. Lemmon to the corresponding field data.

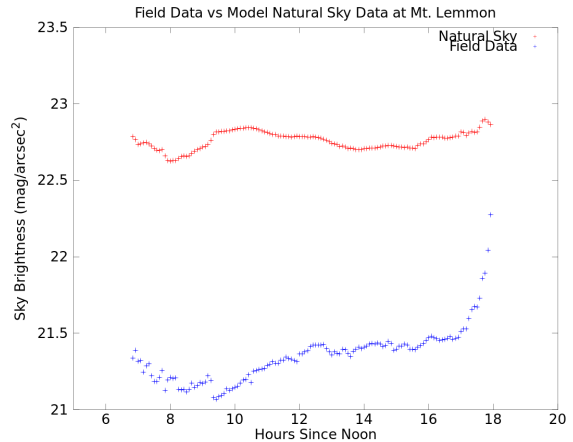


Fig. 9.— Comparison of the modeled natural sky glow (red) and the field data (blue).

As shown in Fig. 9, the anthropogenic contribution to sky glow brightens the sky by as much as 2 mag/arcsec<sup>2</sup> even when the location is as removed at Mt. Lemmon, which is over 61 km away from Tucson.

The TSL237 detector inside the SQM not strictly V band (TAOS (2007)) and the filter inside the meter is not blocking near IR wavelengths (see Table 2). This is a problem since this model calculates sky glow based on V band sky glow. It is also important to note that this model

does not account for the effect of the sun or the moon, causing the determined sky glow to be too dark during twilight and moonlight. Data taken while the moon was up and during sun or moon twilight were not included in the comparison to the model.

### 3.3. Trends

Analysis of temporal trends is done by comparing data from each season, each day of the week, and each month. Further investigation is accomplished via Fourier analysis. Spatial trends are examined by comparing data from the various sites in and around Tucson. To better understand the strength of anthropogenic light contribution, the sites are put into three categories: NOAO (near the center of Tucson), Cardinal Point Sites (four SQMs located in outskirts of the city, each in a cardinal direction), and Observatory Sites (three SQMs located at observatories well outside the city of Tucson). As seen by comparing the graphs in Fig 3, artificial lighting can brighten the sky by as much as 3 mag/arcsec<sup>2</sup>.

To better analyze the periodic features of the sky glow in the Tucson area, a Fourier analysis is undertaken. First, nightly averages of the reduced SQM data are taken and used to generate a time series. The average of this time series is then subtracted and a Hann window function is applied with zero padding. The discrete Fourier transform is computed, and the resulting data are interpolated with a cubic spline method. Converting from the frequency domain to the period domain gives the periodograms in Fig. 11. This process is applied to both raw and reduced data sets. Most of the SQM data collection sites were established in autumn 2012 and were brought in for during the winter for recalibration. Due to the limited amount

of data, the periodograms do not include periodicities greater than 50 days.

The most notable difference between these is the presence of a very strong 28 day period in the raw data, which is less pronounced in the reduced data, illustrating the effect of the moon on sky glow. The increased power of the lunar period for the raw data at sites farther away from Tucson suggests that artificial light greatly decreases the effect of the moon relative to sky glow within Tucson. After data taken while the moon is overhead and during moon twilight are removed, the trend correlated with the moon does not completely disappear. This means that there might also be a relation to the atmospheric tidal effects of the moon. A fifteen day trend found is also correlated to moon twilight and is dependent on distance from Tucson. The fifteen day trend as well as a ten day trend are suggested by the raw and reduced Fourier transforms (Fig. 12), but it is important to note that the amplitudes of these periods are near the noise-level and there may not have significance. Averaged nights of each day of the week are also plotted to analyze variation of light pollution throughout the work week.

Comparisons of the average night per season are made in Fig. 3. Autumn is consistently darker in Tucson by about one mag/arcsec<sup>2</sup>, but there is substantially less variation seen at the observatory sites. To examine seasonal variation in greater detail, SQM readings averaged over 30 day periods are found for the entire data set. These variations were found to correlate strongly with annual-scale variations in 557.7 nm OI airglow intensity. Fig. 10 compares 557.7 nm OI airglow data from Kitt Peak (Smith & Steiger. (1968)) with SQM data taken at the Kitt Peak site. Because the OI 557.7 nm airglow is the

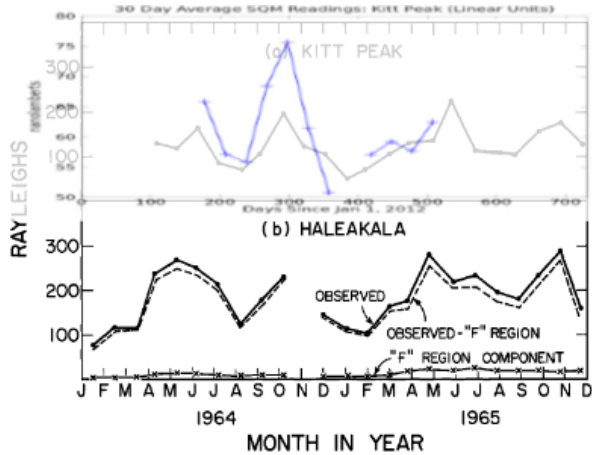


Fig. 10.— SQM data overlaying OI 557.7 nm airglow data at Kitt Peak. The SQM readings were converted to nanolamberts for better comparison to airglow intensity, which is traditionally given in Rayleighs.

brightest airglow emission line in the visual range Baker et al. (1985) and the peak sensitivity of the TSL237 detector is around this wavelength, the OI 557.7 nm line is the most significant photochemical contributor to SQM readings. To obtain a more complete understanding of the role airglow plays in light pollution, future work might include comparisons to other airglow emission lines within the range of the SQM detector.

#### 4. Conclusion

Light pollution is a source of various environmental, economic, and astronomical problems. To better understand light pollution, SQMs have been used to measure sky glow in and around Tucson since June 2012. Wavelength sensitivity tests were done with the SQMs to help interpret these data and revealed that the weatherproof housing affects the readings in a very predictable way. To compensate for how the housing affects the SQM readings, a constant offset can be added to the readings

for each SQM. To minimize the needed offset, the housing will be painted in such a way as to reduce UV yellowing and internal light scatter. A less understood result of laboratory testing of the SQMs is the affect the CM500 filter has on the SQM detector. The filter itself may lay at different angles with each SQM, and the density distribution of plastic in the casing determines what percent of light bypasses the filter altogether.

Newly written and implemented python scripts analyze and reduce the data in a consistent and repeatable way. Data taken when the moon, sun, or Milky Way is up are removed, as are data taken during twilight or moon twilight. There are future plans to implement these scripts into a GUI for the GaN light pollution campaign, in an effort to facilitate citizen science contributions to the field of light pollution study.

The anthropogenic contribution of the reduced data is measured by Dan Duriscoe’s sky brightness model. The difference between the natural sky glow and the field readings (which gives a measure of the anthropogenic sky glow) is typically on the order of one mag/arcsec<sup>2</sup>. This model, however, assumes a constant airglow contribution, which is not the case; the time series of data taken from Kitt Peak showed a strong long term correlation to the annual variation of the OI 557.7 nm airglow.

Several other trends were found in the light pollution in and around Tucson. Both the 28 day and the 15 day trend are correlated with the moon, though the cause of the ten day trend is unknown. Autumn is consistently darker in Tucson, but there is little variation at the observatory sites.

As more data are collected, trends and periodicities of greater length or weaker strength might be identified with greater

confidence. In the meantime, due to the strong correlation of SQM data with the OI 557.7 nm line airglow intensity, other airglow contributions will be investigated - specifically the OI 630.0 nm line and the Na 587.3 nm line. Inconsistencies between SQMs might be further investigated in the laboratory and validation of the SQM data will be pursued via comparison with VIIRS data.

$\lambda$ (nm)	NOAO	East	West	North	South	Kitt Peak	Mt. Hopkins	Mt. Lemmon
365 A	20.27±0.000	20.25±0.008	20.23±0.005	20.26±0.005	20.23±0.000	20.26±0.005	20.27±0.000	20.24±0.006
365 B	20.15±0.009	20.15±0.000	20.12±0.008	20.14±0.000	20.11±0.008	20.13±0.000	20.14±0.010	20.12±0.000
470 A	19.78±0.009	19.75±0.005	19.74±0.000	19.75±0.010	19.74±0.014	19.75±0.000	19.75±0.009	19.73±0.006
470 B	19.66±0.000	19.63±0.008	19.61±0.000	19.64±0.008	19.62±0.010	19.62±0.008	19.64±0.009	19.61±0.008
570 A	18.60±0.000	18.56±0.006	18.69±0.010	18.60±0.000	18.71±0.006	18.58±0.012	18.58±0.008	18.73±0.010
570 B	18.62±0.005	18.57±0.000	18.52±0.011	18.48±0.010	18.52±0.010	18.47±0.009	18.50±0.012	18.51±0.009
655 A	19.91±0.005	19.90±0.000	20.25±0.008	20.07±0.009	19.97±0.000	20.08±0.006	20.03±0.010	20.15±0.010
655 B	19.65±0.015	19.71±0.010	20.03±0.000	19.82±0.012	19.82±0.010	19.93±0.006	19.77±0.005	19.99±0.000
770 A	19.68±0.010	19.62±0.010	20.22±0.000	19.90±0.000	19.87±0.010	19.90±0.000	19.80±0.010	20.06±0.000
770 B	19.43±0.000	19.54±0.000	20.19±0.000	19.67±0.008	19.60±0.012	19.70±0.010	19.55±0.010	19.87±0.040
850 A	20.13±0.010	20.13±0.005	20.72±0.006	20.40±0.005	20.29±0.006	20.40±0.000	20.35±0.010	20.51±0.009
850 B	19.92±0.012	19.92±0.000	20.50±0.010	20.04±0.009	20.08±0.008	20.20±0.000	20.15±0.010	20.35±0.014
950 A	20.07±0.008	20.10±0.013	20.67±0.000	20.34±0.006	20.27±0.011	20.37±0.010	20.29±0.008	20.48±0.000
950 B	19.90±0.006	20.13±0.017	20.46±0.010	20.08±0.010	20.04±0.006	20.14±0.008	20.11±0.028	20.24±0.010

Table 2: Wavelength sensitivity data for SQMs with and without glass filter and housing (A and B resp.) in mag/arcsec<sup>2</sup>.

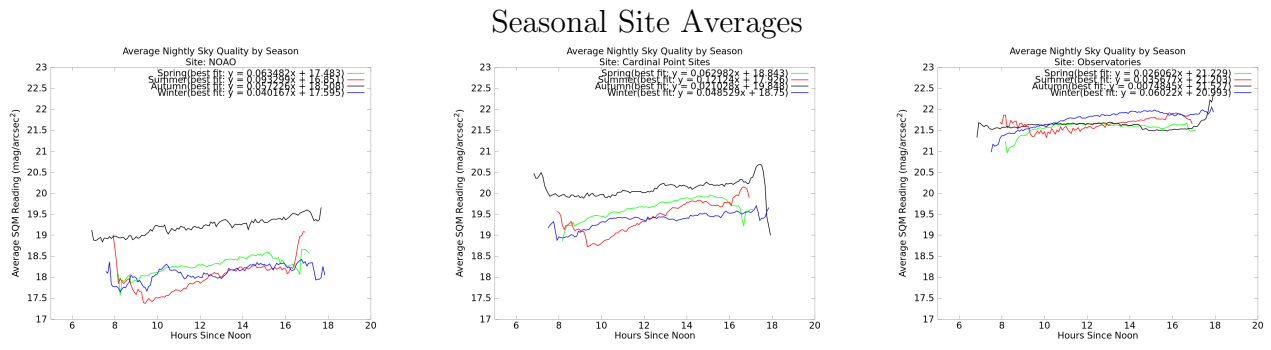


Table 3: Seasonal comparison plots of NOAO, Cardinal Point Sites, and Observatory Sites.

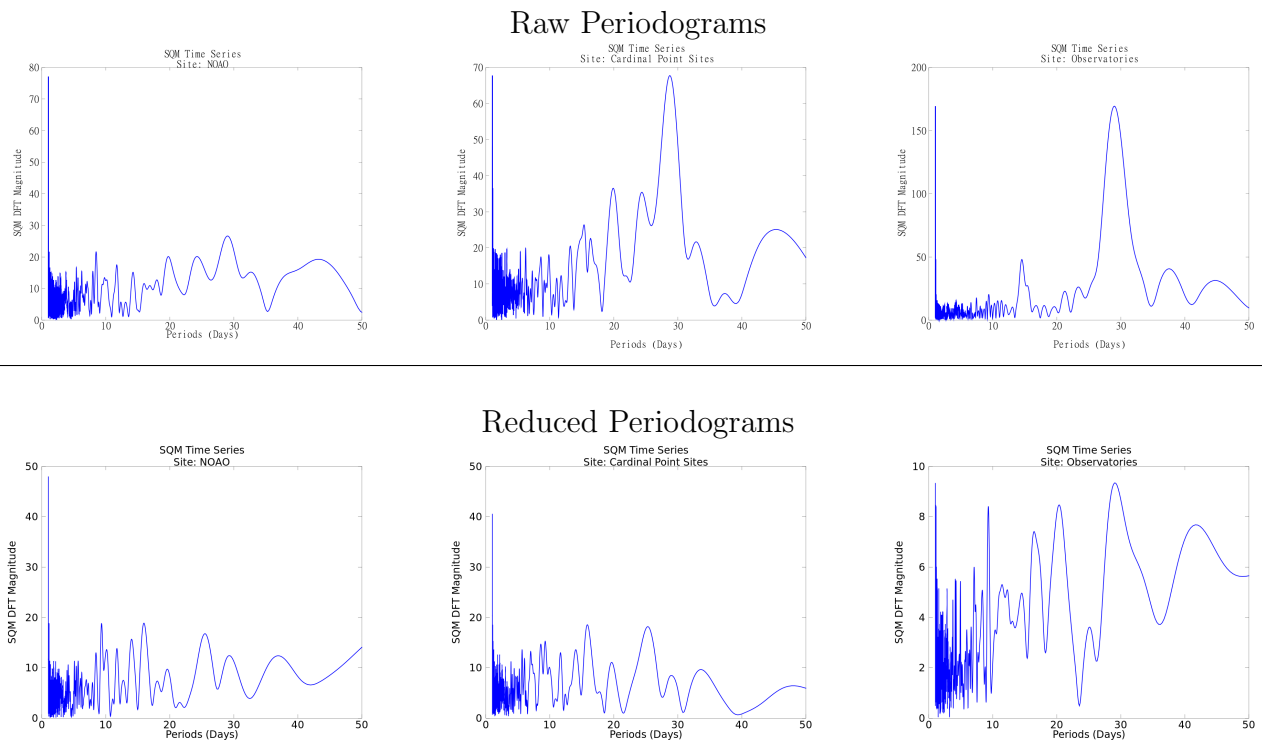
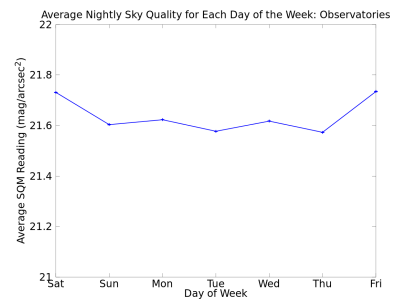
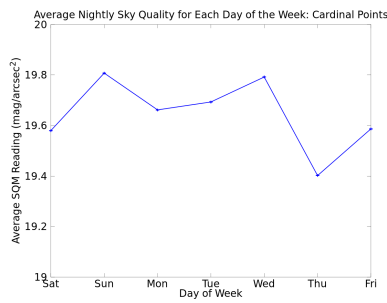
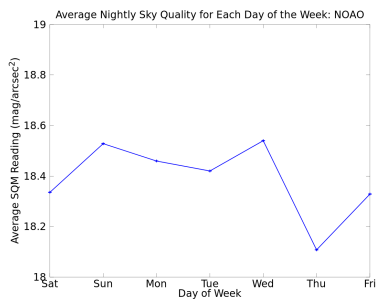


Fig. 11.— Periods in nightly averaged SQM readings at NOAO, Cardinal Point Sites, and Observatory Sites before and after reduction.

### Seven Day Trends



### Ten Day Trends

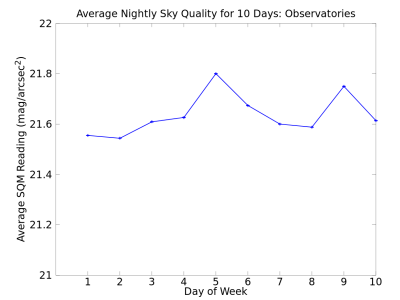
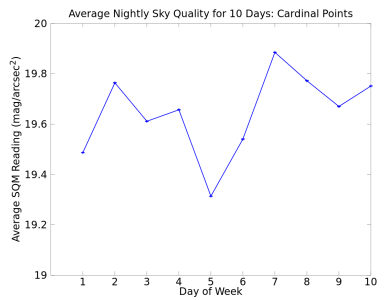
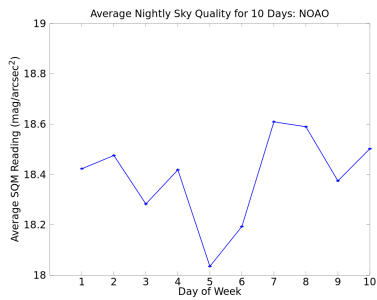


Fig. 12.— Temporal trends for NOAO, Cardinal Point Sites, and Observatory Sites.

## REFERENCES

- Baker, D. J., et al. 1985, Ground-based atmospheric infrared and visible emission measurements.
- Duriscoe, D. M. 2013, Measuring anthropogenic sky glow using a natural sky brightness model.
- Hansen, J. 2001, Increased breast cancer risk among women who work predominantly at night., danish Cancer Society, Institute of Cancer Epidemiology, Copenhagen.
- Hoya-Optics. 2008, Color Compensating Filter (Cyan) CM-500
- Navara, K. J., & Nelson., R. J. 2007, The dark side of light at night: physiological, epidemiological, and ecological consequences.
- Smith, L. L., & Steiger., W. 1968, Night Airglow Intensity Variations in the [O I] 5577 A, [O I] 6300 A, and NaI 5890-96 A Emission Lines.
- TAOS. 2007, TSL237 High-Sensitivity Light-to-Frequency Converter
- Unihedron. 2013, Sky Quality Meter – Lens USB - Datalogger SQM-LU-DL User manual